Research Article

A Brain-Permeable Aminosterol Regulates Cell Membranes to Mitigate the Toxicity of Diverse Pore-Forming Agents

Ryan P. Kreiser,[⊥] Aidan K. Wright,[⊥] Liam R. Sasser,[⊥] Dillon J. Rinauro, Justus M. Gabriel, Claire M. Hsu, Jorge A. Hurtado, Tristan L. McKenzie, Silvia Errico, J. Alex Albright, Lance Richardson, Victor A. Jaffett, Dawn E. Riegner, Lam T. Nguyen, Kathleen LeForte, Michael Zasloff, Jared E. Hollows, Fabrizio Chiti, Michele Vendruscolo,* and Ryan Limbocker*

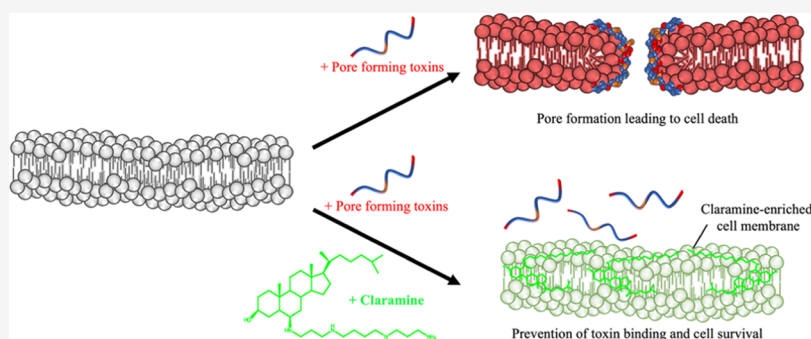Cite This: ACS Chem. Neurosci. 2022, 13, 1219−1231

Read Online

ACCESS | Metrics & More | Article Recommendations | Supporting Information

ABSTRACT: The molecular composition of the plasma membrane plays a key role in mediating the susceptibility of cells to perturbations induced by toxic molecules. The pharmacological regulation of the properties of the cell membrane has therefore the potential to enhance cellular resilience to a wide variety of chemical and biological compounds. In this study, we investigate the ability of claramine, a blood−brain barrier permeable small molecule in the aminosterol class, to neutralize the toxicity of acute biological threat agents, including melittin from honeybee venom and α-hemolysin from *Staphylococcus aureus*. Our results show that claramine neutralizes the toxicity of these pore-forming agents by preventing their interactions with cell membranes without perturbing their structures in a detectable manner. We thus demonstrate that the exogenous administration of an aminosterol can tune the properties of lipid membranes and protect cells from diverse biotoxins, including not just misfolded protein oligomers as previously shown but also biological protein-based toxins. Our results indicate that the investigation of regulators of the physicochemical properties of cell membranes offers novel opportunities to develop countermeasures against an extensive set of cytotoxic effects associated with cell membrane disruption.

KEYWORDS: *biotoxin neutralization, aminosterols, steroid polyamines, cell membranes, cellular resistance, pore-forming agents*

■ INTRODUCTION

Cell homeostasis is critically dependent on the integrity of the plasma membrane, a key cellular structure that acts as a barrier to separate the intracellular and extracellular spaces and as a conduit for extracellular and intracellular signaling pathways.[1−4] Damage to cell membranes results in the aberrant influx and efflux of messengers and metabolites and also results in damaging oxidative stress as an attempt to repair this dysfunction and other aberrant activations. This can be corrected by evolutionarily conserved responses to restore membrane integrity. Failures of these repair mechanisms can play a key role in the onset and development of a variety of acute and chronic pathologies, such as skeletal myopathies, cardiac muscle injury, migration-induced injuries in cancer cells during invasion and metastasis, pore-mediated injuries from immune cells and cytolysins, neuronal membrane damage

during aging, traumatic brain injuries, and neurodegenerative disease.[2] Cell survival in the presence of biological threat agents, ranging from exogenously delivered toxins to endogenously formed protein misfolded aggregates, is therefore critically dependent on the maintenance of key properties of the plasma membrane.
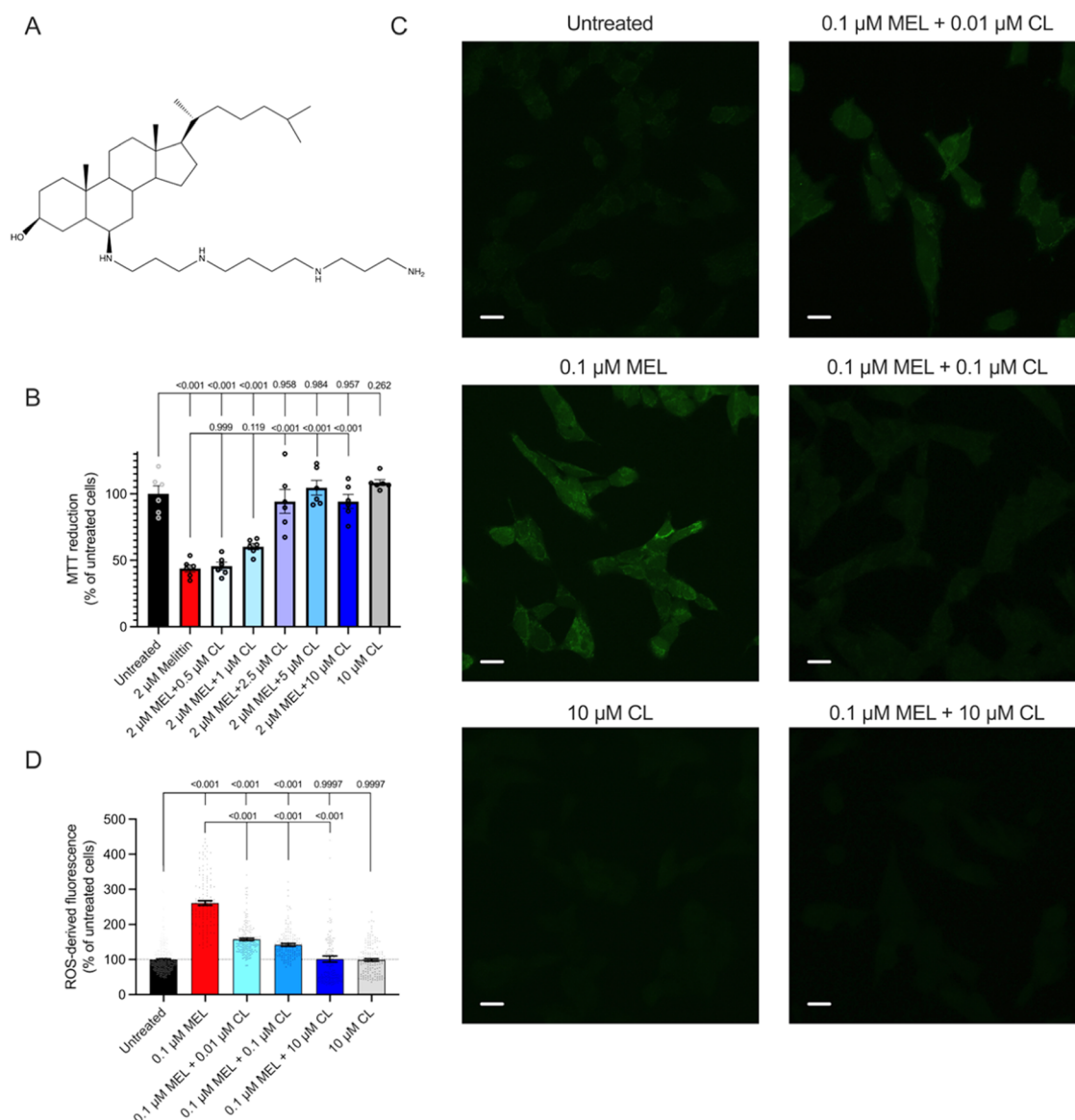
Lipids, including fatty acids, glycerolipids, glycerophospholipids, sphingolipids, sterol lipids, prenol lipids, and others,
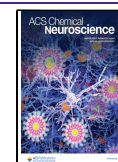
Figure 1. Cytotoxicity induced by the pore-forming peptide melittin is attenuated by claramine. (A) Structure of claramine. (B) 3-(4,5-Dimethylthiazol-2-yl)-2,5-diphenyltetrazolium bromide (MTT) viability assays after cells were exposed to 2 μM melittin (MEL) in the absence (red bar) or presence of increasing concentrations of claramine (CL, blue bars) for 20 h. Cells were also exposed to 10 μM claramine alone (gray bar). The physiological range of claramine under these conditions is shown in Figure S1A. n = 60,000 cells per condition corresponding to the six technical replicates shown. Conditions were analyzed by one-way analysis of variance (ANOVA) followed by Dunnett's multiple comparison test relative to untreated cells or cells treated with melittin, as indicated. Untreated cells and cells treated with 10 μM claramine were analyzed by an unpaired, two-tailed Student's t-test. Data are representative of n = 3 biologically independent experiments. (C) To study the acute effects of melittin treatment, 0.1 μM melittin was incubated with cells for 5 min in the absence or presence of increasing concentrations of claramine (0.01–10 μM). Cells were also treated with 10 μM claramine in the absence of melittin. The fluorescence of the 6-chloromethyl-2′-7′-dichlorodihydrofluorescein diacetate (CM-H$_2$DCFDA) general oxidative stress indicator was used to measure the extent of reactive oxygen species (ROS) production in various conditions. A superimposition of 1.0 μm thick sections spanning the height of the entire cell was compiled to generate the shown representative images. Scale bars, 10 μm. Enhanced contrast and brightness images can be seen in Figure S9, which show clearly all cells, including those with a low fluoresce signal. (D) Corresponding semiquantitative values of green fluorescence. All samples were analyzed by one-way ANOVA followed by Dunnett's multiple comparison test relative to untreated cells. Samples containing melittin and claramine were analyzed by one-way ANOVA followed by Dunnett's multiple comparison test relative cells treated with melittin alone. Bars indicate mean ± standard error of the mean (s.e.m.) of at least 130 cells per condition.

make up approximately 50% of the dry brain weight[5] and are a fundamental component of neuronal cell membranes. Extensive evidence shows that dysfunction in lipid homeostasis as a result of aging or pathology is associated with neurologic disorders and neurodegenerative diseases.[4,6−11] Therefore, modulation of the cell membrane with therapeutic compounds has the potential to promote the resilience of neurons against a

wide variety of threat agents by controlling the lipid composition of the plasma membrane.

In the search for these therapeutic compounds, we have previously shown that trodusquemine, a representative aminosterol, localizes within the hydrophilic region of the lipid bilayer and extends to the interface between the hydrophilic and hydrophobic regions with a well-defined oblique angle

(about 55°) for the major axis of the molecule with respect to the normal to the bilayer plane and with superficial positioning of its positively charged spermine tail.[12] As a result, the membrane becomes less negatively charged, protected against oligomer embedding, and it causes a redistribution of cholesterol and ganglioside GM1 molecules that are known to protect cells from oligomer toxicity.[12] Given the observations of a conserved mechanism of action of the aminosterols against aggregates, including multiple types of protein misfolded oligomers,[13−22] we hypothesized that they could act as a regulator of the cell membrane to suppress the toxicity of a wide range of different threat agents.

In particular, we studied herein the pore-forming agents melittin (MEL) and α-hemolysin (α-HEM). Monomeric melittin readily interacts with phospholipids in the plasma membrane to form approximately 4.4 nm transmembrane pores that can induce membrane permeabilization and cell death.[23−26] Melittin is the active component of honeybee venom, and this positively charged, 2.85 kDa, amphipathic 26-amino acid peptide exhibits a random coil structure and transforms into an α-helix upon binding to membranes, where the helical monomer has two helical segments joined by a coiled region containing a proline.[23,27] This antimicrobial peptide has been studied extensively for its antitumoral effects in a variety of cancers.[23] The significantly larger pore-forming agent α-hemolysin is 33.2 kDa in its monomeric form and 232.4 kDa when adopting its homo-heptameric state.[28] Hemolysins are produced by bacterial and fungal pathogens and have the ability to lyse erythrocytes, monocytes, lymphocytes, and macrophages by hydrolyzing or forming pores in the phospholipid bilayers of cell membranes.[29−31] The pores created by hemolysin lead to the uncontrolled exchange of monovalent ions resulting in DNA fragmentation and cell death. In its functional self-assembled state, α-hemolysin, in particular, is a homo-heptameric β-barrel pore-forming protein produced by *Staphylococcus aureus* that is both hemotoxic and neurotoxic due to its ability to lyse isolated nerve endings and astrocytes.[32,33] In addition to these toxins, other peptides can induce pore formation, such as the antimicrobial peptide NK-2 from the cationic core of NK-lysin. In this case, electrostatic interactions between NK-2 and anionic lipid membranes appear to mediate binding affinity, which has relevance to the development of new antibiotics.[34]

In this work, we show that the aminosterol claramine (CL) (Figure 1A), a low cost, commercially available steroid polyamine similar in structure to the natural products squalamine and trodusquemine, protects human neuroblastoma (SH-SY5Y) cells from the pore-forming agents melittin and α-hemolysin by inhibiting the binding of these biomolecules to cell membranes. As observed for protein misfolded oligomers and other aminosterols,[18] this protective mechanism of claramine occurred without overt changes to the structures of monomeric melittin or α-hemolysin. These findings therefore suggest that aminosterols can regulate cell membranes to protect neuronal cells from highly diverse biological toxins, including small and large pore-forming peptides and proteins, as well as protein misfolded oligomers. Taken together, our results indicate that this therapeutic approach may be relevant to the rational design of countermeasures against biological threat agents and pathologies associated with cell membrane dysfunction, such as muscular dystrophies, cardiac muscle injuries, metastatic cancers, traumatic brain injuries, antibiotic resistance, and numerous other protein misfolding diseases.

RESULTS

Claramine Neutralizes the Toxicity of Melittin. To investigate the ability of claramine to neutralize potent toxins, we began by studying its impact on the pore-forming peptide melittin. We first exposed SH-SY5Y human neuroblastoma cells to increasing concentrations of claramine for 20 h (Figure S1A), finding that concentrations at and below 10 μM in cell culture media did not impact the viability of the cells, as quantified using the MTT reduction cell viability assay.[13] Similarly, we treated the cells with increasing concentrations of melittin under the same conditions, finding that 2 μM induced a clear and significant drop in cell health to 51 ± 3% of untreated cells (mean ± standard error of the mean, s.e.m.) and that toxicity increased further at 5 μM with a cell viability of 8 ± 1% of untreated cells (Figure S1B). Cells were then exposed to 2 μM melittin and increasing concentrations of claramine ranging from 0.5 to 10 μM (Figure 1B), for which a clear, dose-dependent decrease in melittin toxicity was observed. Indeed, cell viability was decreased to 44 ± 3% (mean ± s.e.m.) of untreated cells upon melittin treatment, while cells treated with melittin and 10 μM claramine had a viability of 94 ± 5% of untreated cells. We also found that claramine could still significantly prevent the toxicity of 4 μM melittin, despite the heightened state of cellular stress at this higher melittin concentration (Figure S1C). With respect to this treatment paradigm, we note that aminosterols are known to bind rapidly within seconds to the cell membrane,[12] whereas the toxicity observed in the MTT assays is only detectable after minutes to hours, as demonstrated herein and previously.[13−15,18,19]

Next, adherent cells exposed to 2 μM melittin for 20 h exhibited a reduced density on the multiwell surface (Figure S2), illustrating its toxic effects toward cells under these conditions. The reduced number of cells observed upon melittin treatment is likely to be a function of attenuated differentiation due to cell stress during the incubation period, cell lysis, or both. Coincubation of the cells with 2 μM melittin and 10 μM claramine prevented the readily observable toxic effects of melittin. Cells were also exposed to 10 μM claramine alone, for which no visible changes in morphology were observed relative to untreated cells exposed to cell media alone (Figure S2). To further explore the kinetics of melittin toxicity, detached cells were exposed to 4 μM melittin in the absence or presence of 5 or 10 μM claramine. At 10 and 40 min of treatment, the integrity of the cell membrane was explored using the trypan blue cell viability assay. In agreement with the MTT and brightfield measurements, claramine preserved membrane integrity and prevented trypan blue inclusion in the cells with a well-defined dose dependence (Figure S3).

To gain further insight into the acute effects of melittin treatment on SH-SY5Y cells, we next performed reactive oxygen species (ROS) measurements. An increase in ROS production is typically more rapid and intense than the decrease of MTT reduction, and we therefore explored lower concentrations of melittin in this more sensitive assay. Cells were treated for 5 min with 0.1 μM melittin in the absence or presence of 0.01−10 μM concentrations of claramine, and the extent of ROS production was assessed using 6-chloromethyl-2′-7′-dichlorodihydrofluorescein diacetate (CM-H$_2$DCFDA) and quantified by confocal microscopy (Figure 1C,D). Melittin
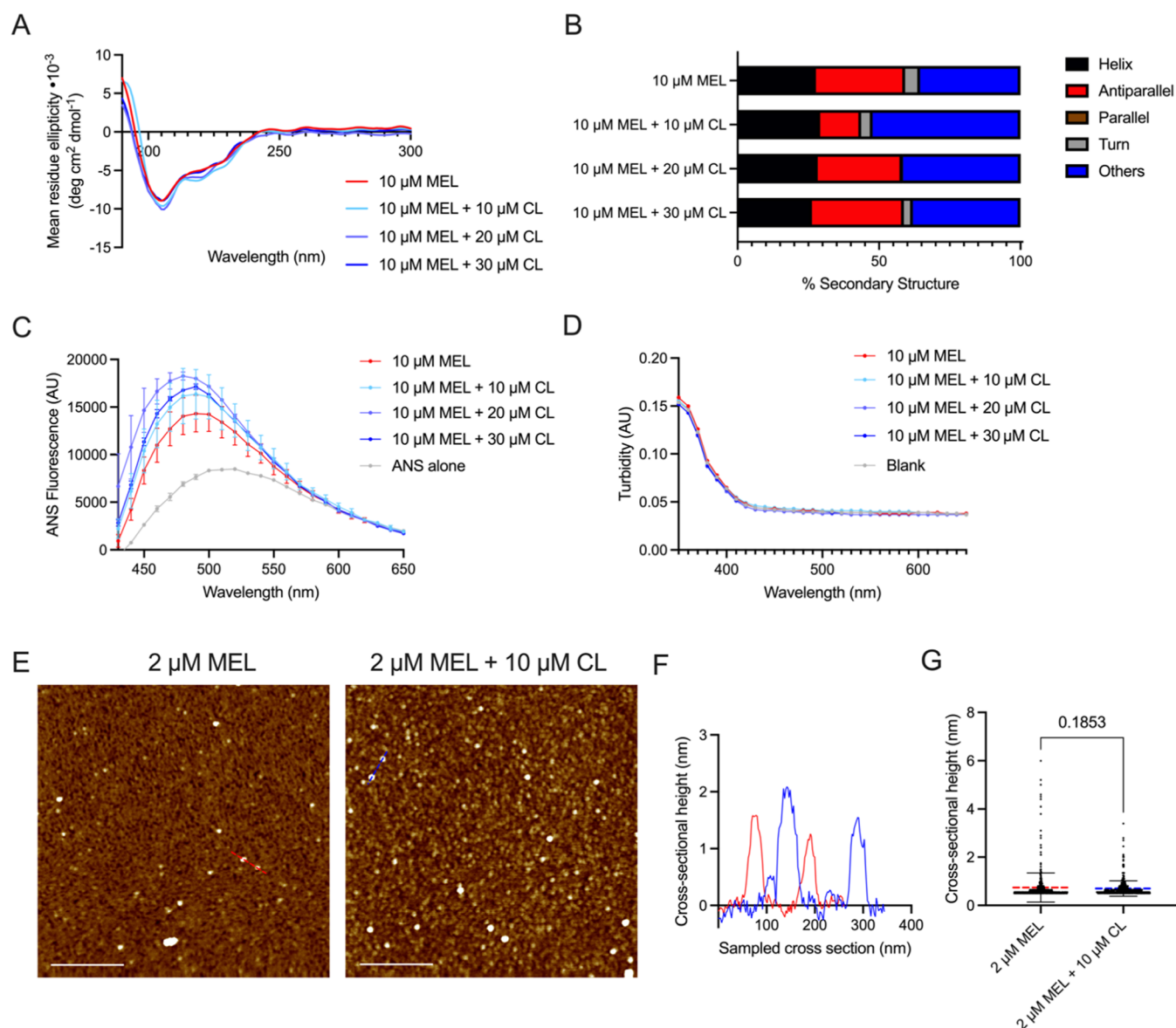
Figure 2. The physicochemical properties of hydrophobicity and size for melittin are not changed by claramine. (A) CD spectroscopy measurements for 10 μM melittin in the absence (red trace) and presence of up to 30 μM claramine (CL, blue traces). Smoothed data are shown. (B) BeStSel-quantified secondary structures for the traces shown in (A). Statistically significant differences were not observed for the samples containing claramine relative to melittin alone ($P > 0.999$ by two-way ANOVA, main row effect). (C) 10 μM melittin was incubated with up to 30 μM concentrations of claramine, after which time 30 μM 8-anilino-1-naphthalenesulfonic acid (ANS) was added to probe the solvent-exposed hydrophobicity of melittin. Free ANS is shown for reference (gray). Error bars indicate the s.e.m. of duplicate technical replicates. Data shown are representative of $n = 2$ independent experiments. (D) Turbidity absorbance measurements for 10 μM melittin incubated with up to 30 μM claramine for the samples shown in (C). (E) Melittin was incubated in the absence and presence of a 5-fold excess of claramine and measured using atomic force microscopy (AFM). Scale bars, 500 nm. (F) Representative cross-sectional heights are shown (red, melittin; blue, melittin + claramine; $n = 500$ per condition), as indicated in the color plots of (E). (G) Quantification of the entire sample population. Line and error bars represent mean ± 1 standard deviation. Data were analyzed using an unpaired, two-tailed Student's t-test. In (A)−(F), all samples were prepared in 20 mM sodium phosphate buffer at pH 7.4.

induced a significant increase in ROS production ($260 \pm 1\%$ of untreated cells, mean $\pm$ s.e.m.) that was dose-dependently attenuated by claramine, where cells treated with 0.1 μM melittin and 10 μM claramine exhibited comparable ROS levels to untreated cells ($101 \pm 1\%$ of untreated cells) and to cells exposed only to 10 μM claramine ($99 \pm 1\%$ of untreated cells) (Figure 1D). Collectively, these data indicate that claramine can neutralize the toxicity of melittin toward SH-SY5Y cells.

Physicochemical Properties of Melittin Are Not Changed by Claramine. In our previous work, we found that the aminosterol trodusquemine did not impact the physicochemical properties of protein misfolded oligomers at physiological concentrations, which in its case was also at or below 10 μM.[18] The ability of trodusquemine and other aminosterols to prevent oligomer toxicity was therefore attributed primarily to its ability to displace or prevent the binding of these toxic proteins from cell membranes.[13−15,18,19] In light of these previous studies and considering that melittin
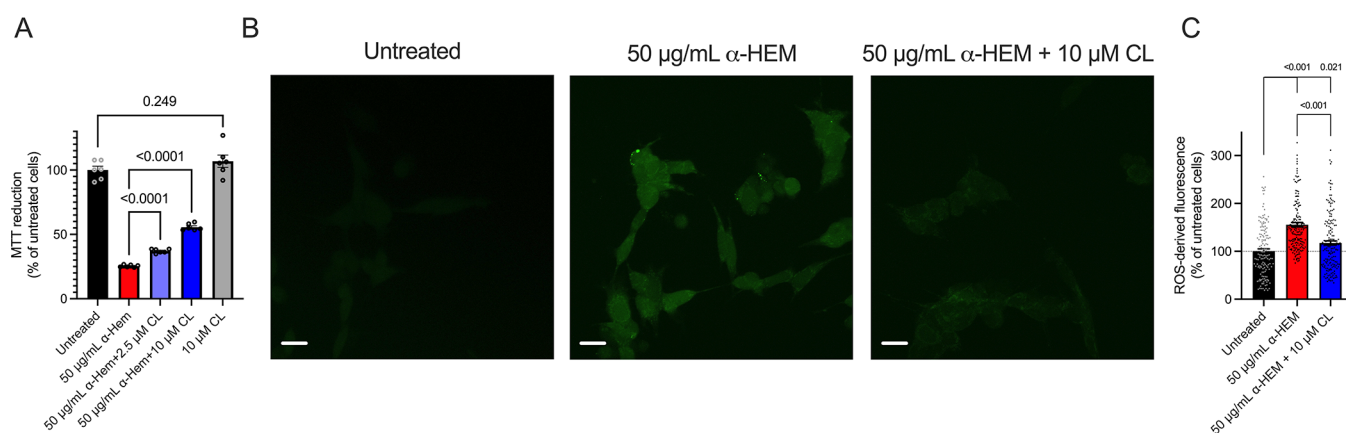
Figure 3. Cytotoxicity induced by the pore-forming peptide α-hemolysin is attenuated by claramine. (A) MTT viability assays after cells were exposed to 50 μg/mL α-hemolysin (α-HEM) in the absence (red) or presence of increasing concentrations of claramine (CL, blue bars) for 20 h. Cells were also exposed to 10 μM claramine alone (gray). n = 60,000 cells per condition corresponding to the shown six technical replicates. Conditions were analyzed by one-way ANOVA followed by Dunnett's multiple comparison test relative cells treated with α-hemolysin or Student's t-test, as indicated. Data shown are representative of n = 3 biologically independent experiments. (B) 50 μg/mL α-hemolysin was incubated with cells for 1 min in the absence or presence of 10 μM claramine. The fluorescence of the CM-H$_2$DCFDA general oxidative stress indicator was used to measure the extent of ROS production. A superimposition of 1.0 μm thick sections spanning the height of the entire cell was compiled to generate the shown representative images. Scale bars, 10 μm. Enhanced contrast and brightness images can be seen in Figure S9, which show clearly all cells, including those with a low fluoresce signal. (C) Corresponding semiquantitative values of green fluorescence. Conditions were analyzed by one-way ANOVA followed by Dunnett's multiple comparison test relative cells treated with α-hemolysin or Student's t-test, as indicated. Bars indicate mean $\pm$ s.e.m. of at least 130 cells per condition.

must first adopt the α-helical structure on the cell surface to induce its membrane-penetrating ability, we predicted that claramine was acting on the cell membrane to prevent melittin toxicity rather than acting on the structure of the toxin directly. We therefore carried out a variety of measurements to quantify the structural and morphological properties of monomeric melittin in the presence of claramine.

First, 10 μM melittin was incubated in the absence or presence of 10–30 μM claramine and the resulting samples were measured using circular dichroism (CD) spectroscopy. The CD spectrum of melittin had a minimum at 205 nm and a shoulder at 215–230 nm, indicating a largely unstructured peptide with elements of residual secondary structures (Figure 2A). We observed that the spectrum was largely unchanged in the presence of claramine (Figure 2A). Similarly, the β structure selection (BeStSel) analysis[35,36] of the spectra demonstrated that the secondary structure composition of melittin was largely unchanged in the presence of increasing concentrations of claramine (Figure 2B). Two-way ANOVA analysis found no significant differences between the secondary structure compositions of melittin without claramine and any of the samples of melittin with varying concentrations of claramine.

For misfolded protein oligomers, small size and solvent-exposed hydrophobicity are well-characterized determinants of cytotoxicity.[37] This is because more hydrophobic assemblies can embed and incorporate readily into the plasma membrane, and smaller ones diffuse more frequently to the cell surface.[37–39] It follows by the same rationale that monomeric pore-forming proteins, or assemblies thereof that could be induced by claramine, might incorporate with the cell membrane more frequently if they become more hydrophobic or smaller. As such, we assessed the solvent exposed hydrophobicity of melittin in the absence or presence of increasing concentrations of claramine using the 8-anilino-1-naphthalenesulfonic acid (ANS) binding assay. In agreement with the observation that melittin has a hydrophobic N-

terminal region, we observed that 10 μM peptide induced a blue shift and increase in its fluorescence intensity relative to the unbound dye, indicating ANS binding (Figure 2C). Concentrations of claramine up to 30 μM in the presence of melittin were not observed to significantly impact the extent of ANS binding, indicating that the molecule is not likely changing the solvent-exposed hydrophobicity of the peptide under these conditions (Figure 2C).

To determine the size of melittin in the absence and presence of claramine, the same samples measured in the ANS assay were also subjected to turbidity absorbance measurements. Increasing concentrations of claramine up to 30 μM did not clearly impact the absorbance signal of melittin, indicating the absence of peptide aggregation (Figure 2D). We also performed atomic force microscopy (AFM) measurements of 2 μM melittin in the absence and presence of 10 μM claramine (Figure 2E–G). The cross-sectional height of melittin was 0.7 $\pm$ 0.1 nm (mean $\pm$ s.e.m.) in the absence of claramine (n = 500) and 0.7 $\pm$ 0.1 nm in its presence (n = 500), which was not significantly different (P = 0.185 by an unpaired, two-tailed Student's t-test) and is typical of a distended nonaggregated polypeptide chain. Overall, the CD, ANS, turbidity, and AFM measurements collectively indicate that claramine does not change the structure and monomeric state of melittin under these conditions.

Claramine Neutralizes the Toxicity of α-Hemolysin without Changing Its Structure. To further investigate the mechanism of action for claramine, we next utilized a significantly larger pore-forming protein in the form of α-hemolysin. We first incubated SH-SY5Y cells with 50 μg/mL (corresponding to approximately 1.5 μM in monomer equivalents) α-hemolysin in the absence or presence of increasing concentrations of claramine up to a maximal dose of 10 μM for 20 h. Cells were analyzed using the MTT assay. Similar to our results for melittin, claramine significantly reduced the toxicity of α-hemolysin in a dose-dependent manner (Figure 3A). Specifically, cell viability was increased
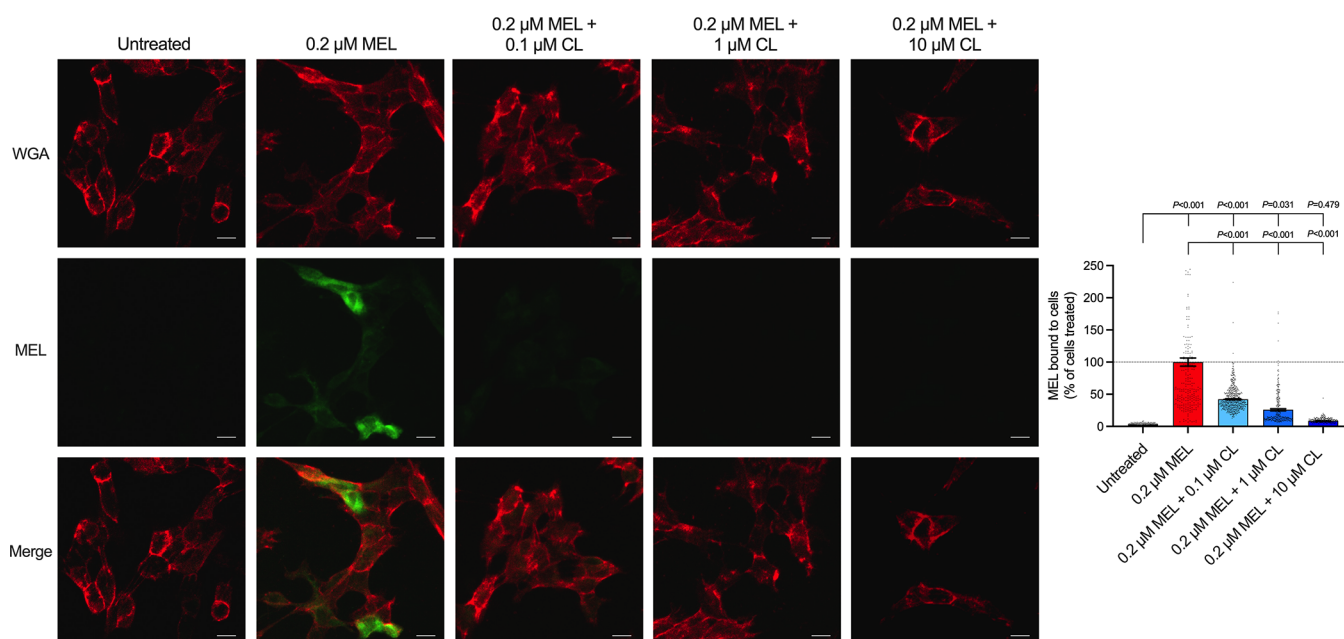
Figure 4. Claramine attenuates melittin binding to cell membranes. SH-SY5Y cells were treated for 5 min with 0.2 μM melittin (MEL) in the absence (red bar) or presence of 0.1, 1.0, or 10 μM claramine (CL, blue bars). Untreated cells exposed only to cell culture media are shown for comparison (black bar). Red and green fluorescence correspond to the cell membrane labeled with wheat germ agglutinin (WGA) and the Alexa 488-labeled melittin, respectively. The bar plot shows the colocalization of melittin with the cell membrane. Scale bars, 10 μm. All samples were analyzed by one-way ANOVA followed by Dunnett's multiple comparison test relative to untreated cells. Samples containing melittin and claramine were analyzed by one-way ANOVA followed by Dunnett's multiple comparison test relative cells treated with melittin alone. Bars indicate mean $\pm$ s.e.m. of at least 200 cells per condition. Data shown are representative of n = 3 biologically independent experiments.

from 25 $\pm$ 1% with α-hemolysin in the absence of claramine to 56 $\pm$ 1% with α-hemolysin in the presence of 10 μM claramine (P < 0.0001, unpaired, two-tailed Student's t-test). Brightfield images taken after cells were incubated with α-hemolysin illustrated significant cellular detachment under these conditions, which was prevented upon the addition of increasing concentrations of claramine, where cells treated with α-hemolysin and 10 μM claramine were similar to untreated cells (Figure S4). Finally, cells treated for 1 min with 50 μg/mL α-hemolysin in the absence and presence of 10 μM claramine were measured for the extent of ROS-derived fluorescence (Figure 3B). As was observed for melittin, α-hemolysin increased the ROS levels in SH-SY5Y cells and claramine reduced the levels of cellular stress (Figure 3C). In all of our quantitative cytotoxicity assays, claramine demonstrated an enhanced efficacy toward neutralizing melittin in comparison to α-hemolysin, which is likely attributed to differences in their mechanisms of action, as discussed in the following section.

We then carried out the MTT assay using identical conditions, as previously described, but with only 30 min of treatment rather than 20 h. Even under this short treatment paradigm, these concentrations of melittin and α-hemolysin were clearly toxic to SH-SY5Y cells, and this toxicity was significantly neutralized by claramine with dose dependence (Figure S5). These findings are consistent with a previous study where HeLa cells were treated with melittin for 6, 12, and 24 h and similar MTT reduction readouts were quantified at each time point across multiple concentrations. A comparison of this work with our findings herein highlights that different cell lines exhibit variable susceptibilities to toxic agents, as comparable reductions in cell viability were observed toward their HeLa cells treated for 24 h with 2 μg/mL

(approximately 0.7 μM) melittin[40] and our SH-SY5Y cells treated for 20 h with 2 μM melittin.

To ensure that the ability of claramine to neutralize the toxicity of melittin is not specific to SH-SY5Y cells, we next cultured and exposed HEK293 human embryonic kidney cells to 2.5 μM melittin in the absence or presence of 2.5−20 μM claramine. HEK293 cells could tolerate 20 μM claramine under these conditions without observable changes to the viability of the kidney cells. The toxicity of melittin was decreased with a well-defined dose dependence by claramine in HEK293 cells (Figure S6), in excellent agreement with the results on SH-SY5Y cells.

As carried out for melittin, we next sought to assess if claramine impacts the structure of monomeric α-hemolysin. Analogous to the case for melittin, 100 μg/mL α-hemolysin interacted with ANS and induced a blue shift and increase in its fluorescence, and increasing concentrations of claramine up to 30 μM exerted a minimal impact on the intensity or wavelength of maximum ANS fluorescence (Figure S7A). Turbidity measurements were also performed with identical concentrations of α-hemolysin and claramine, and the size of α-hemolysin was not overtly changed by increasing concentrations of claramine (Figure S7B). These measurements suggest that claramine does not impact the structure and aggregation state of monomeric α-hemolysin.

Claramine Attenuates the Binding of the Pore-Forming Agents to Cell Membranes. We next sought to explore further the mechanism by which claramine attenuates the toxicity of the two pore-forming agents explored herein. The biophysical properties of hydrophobicity and size, which can mediate the interactions of oligomeric proteins with cell membranes,[37] were unchanged by physiological concentrations of claramine for melittin and α-hemolysin (Figures 2 and S7).
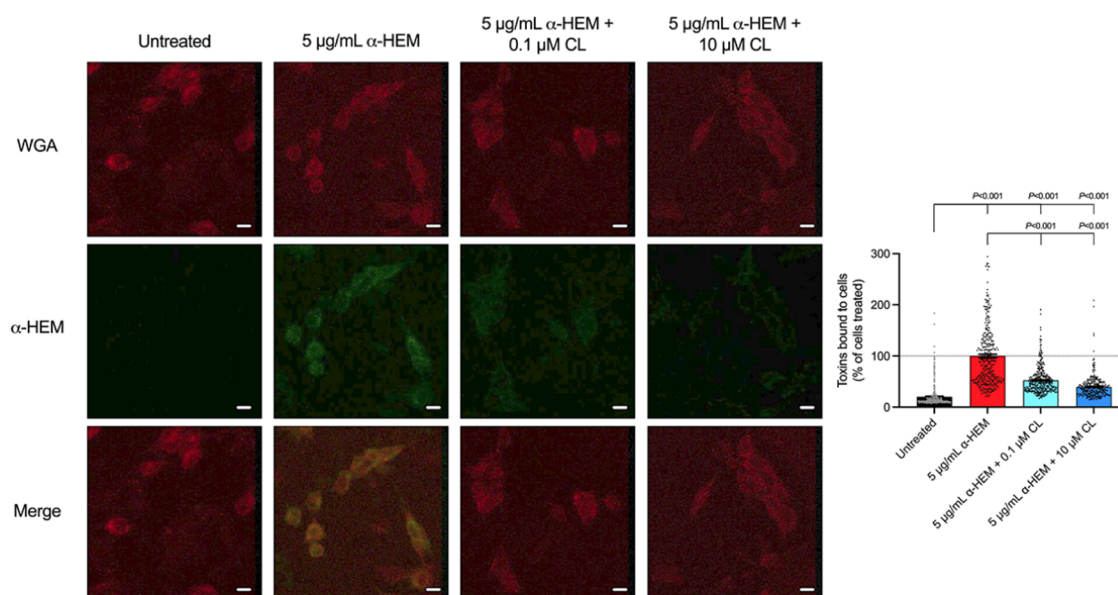
Figure 5. Claramine also reduces α-hemolysin binding to cell membranes. SH-SY5Y cells were treated for 15 min with 5 μg/mL α-hemolysin (α-HEM) in the absence (red bar) or presence of 0.1 or 10 μM claramine (CL, blue bars). Untreated cells exposed only to cell culture media are shown for comparison (black bar). Red and green fluorescence correspond to the cell membrane labeled with wheat germ agglutinin (WGA) and the α-hemolysin protein, respectively. Scale bars, 10 μm. The bar plot shows the colocalization of α-hemolysin with the cell membrane. All samples were analyzed by one-way ANOVA followed by Dunnett's multiple comparison test relative to untreated cells. Samples containing α-hemolysin and claramine were analyzed by one-way ANOVA followed by Dunnett's multiple comparison test relative cells treated with α-hemolysin alone. Bars indicate mean $\pm$ s.e.m. of at least 300 cells per condition. Data shown are representative of $n = 2$ biologically independent experiments.
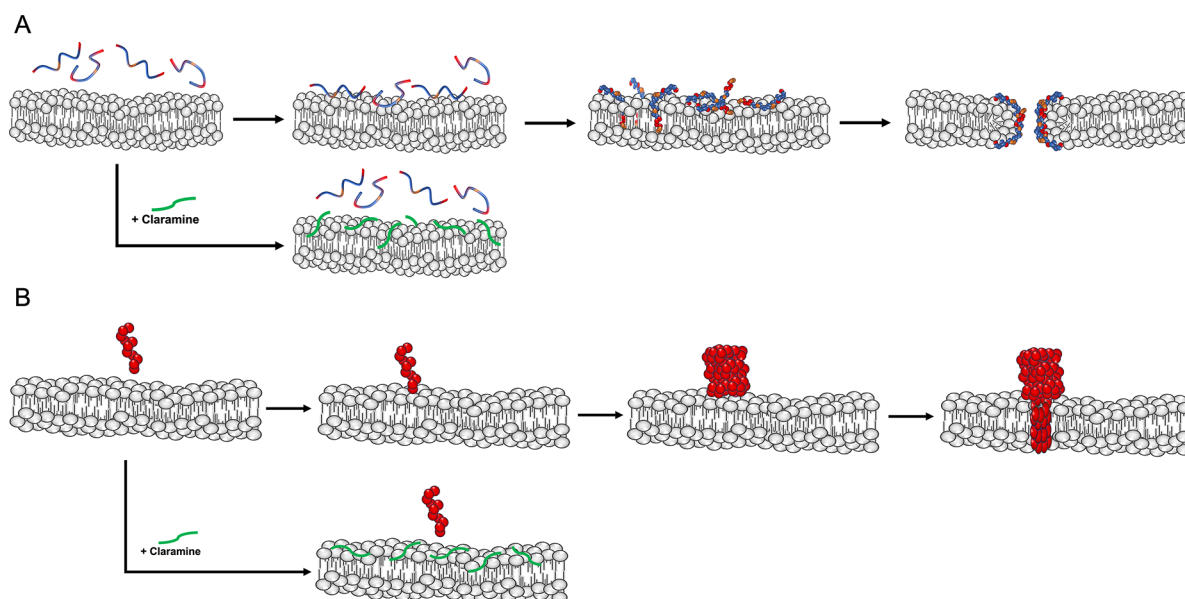
Figure 6. Schematic for the mechanism of action by which the folded toxins melittin (A) and α-hemolysin (B) disrupt and create pores in the cell membranes. The illustration shows how claramine (green) incorporates into the cell membrane to prevent the pore-forming toxins from docking, analogous to the case for protein misfolded oligomers observed in neurodegenerative diseases.[15,16,19,21,22] The graphic was generated from the knowledge that aminosterols localize within the hydrophilic region of the lipid bilayer and extend to the interface between the hydrophilic and hydrophobic regions with a well-defined oblique angle (about 55°) for the major axis of the molecule with respect to the normal to the bilayer plane and with superficial positioning of its positively charged spermine tail.[12] As a result, the membrane becomes less negatively charged, and it causes a redistribution of cholesterol and ganglioside GM1 molecules and acquires resistance to indentation.[12]

It has previously been shown that the extent of binding of misfolded protein oligomers, such as Aβ_{42}, Aβ_{40}, αS, and HypF-N oligomers, to cell membranes is directly related to the toxicity quantified by MTT and ROS assays.[11,13,15] We therefore sought to quantify the interaction of these pore-forming agents with the plasma membranes of SH-SY5Y cells to visualize if the previously observed protective mechanism of aminosterols against misfolded protein oligomers extends to pore-forming peptides and proteins.

To determine the extent of the interaction between melittin and α-hemolysin with cell membranes, we elected to conjugate melittin with the Alexa Fluor 488 succinimidyl ester, whereas a

commercial antibody was available to aid in the visualization of α-hemolysin. Adherent SH-SY5Y cells were treated for 5 or 15 min, respectively, at 37 °C with either 0.2 μM 488-labeled melittin (Figure 4) or 5 μg/mL unlabeled α-hemolysin (Figure 5) in the absence or presence of varying concentrations of claramine, after which they were counterstained with Alexa Fluor 633-conjugated wheat germ agglutinin (WGA, to visualize cell membranes) and fixed. In the case of α-hemolysin, cells were subsequently exposed to the commercially available antistaphylococcal α-toxin primary antibodies and Alexa Fluor 488-conjugated secondary antibodies (Figure 5). For melittin, we verified that its biological activity was not affected by its labeling with the Alexa Fluor 488 succinimidyl ester: cells were exposed to 1, 2, and 4 μM melittin that was either labeled or unlabeled, and MTT viability assays showed that labeling did not change the toxicity of melittin toward SH-SY5Y cells (Figure S8).

Relative to the condition in the absence of any aminosterol, the addition of 0.1 μM claramine to the reaction mixture reduced melittin binding to cell membranes to 42 ± 1%, whereas the addition of 1.0 or 10 μM claramine reduced melittin binding to the plasma membrane to 26 ± 2 and 9 ± 1%, respectively ($P < 0.001$, one-way ANOVA with Dunnett's multiple comparison test relative to cells treated with melittin) (Figure 4). In addition, the binding of α-hemolysin to the cell membrane was reduced to 52 ± 1 and 40 ± 1% of cells treated with α-hemolysin only upon the addition of 0.1 and 10 μM claramine, respectively ($P < 0.001$, one-way ANOVA with Dunnett's multiple comparison test relative to cells treated with α-hemolysin) (Figure 5). The extent of pore-forming peptide binding is in excellent agreement with the viability data, where the binding and toxicity of melittin are nearly completely attenuated upon the addition of 10 μM claramine (Figures 1 and 4), whereas these parameters were only partially reduced in the case of α-hemolysin at commensurate concentrations of the aminosterol (Figures 3 and 5). Collectively, the data support the conclusion that claramine incorporates into the cell membrane and prevents the binding and resultant toxicity of melittin and α-hemolysin (Figure 6), therein extending the generic mechanism of action for aminosterols in protecting cell membranes from protein misfolded oligomers to include small and large pore-forming biotoxins.

■ DISCUSSION

The results that we have reported here illustrate the efficacy of claramine as a countermeasure against the cytotoxicity of pore-forming agents. We have demonstrated that the mechanism by which this aminosterol functions is by attenuating the binding of these toxins to cells, thereby preserving the integrity of the plasma membrane (Figure 6). Analysis of the effects of claramine against melittin and α-hemolysin reveals that claramine is protective through a generic, cell-membrane based mechanism, as it does not alter the physicochemical properties of either toxic agent at the molar ratios used in our experiments.

Melittin is a 2.8 kDa peptide that adopts an α-helical structure upon interaction with cell membranes, which segregates the hydrophobic and hydrophilic residues.[27,41−43] This α-helical character is suggested to be a key factor in the recognition of lipopolysaccharides by melittin in the outer membrane of Gram-negative bacteria, alluding to its antimicrobial properties.[42] Furthermore, in vitro studies of

melittin in the presence of zwitterionic lipids result in two competing modes of action: an inactive, parallel conformation and an active, inserting mode of action.[27] The latter provides for the accessibility of embedding within the lipid membrane, causing pore formation and disrupting membrane integrity, including in epithelial cells and red blood cells.[23,44] α-Hemolysin operates in a similar but more elaborate fashion, owing to its greater structural complexity. Monomeric α-hemolysin interacts with areas of high lipid density on the cellular membrane to form a heptamer on the surface of the lipid membrane.[45] The 232.4 kDa mushroom-shaped toxin contains a 14-membered β-barrel stem with a hydrophobic belt. It measures in at 100 Å in overall height and diameter.[28] As a result, the heptamer can extend a perforating pore into the cellular membrane that is large enough to allow for the passage of small molecules and ions to the exterior of the cell.[46] The large difference in size between melittin and α-hemolysin may offer an explanation for the difference in efficacy observed for claramine against these toxins, where this aminosterol could fully and partially prevent the toxicity of melittin and α-hemolysin, respectively. While claramine proved effective in preventing the toxicity of pore-forming agents to the two unique cell lines explored in this study, it is not known at present if claramine targets certain types of pores, such as toroidal ones.[24]

Although the two toxins act with two different specific mechanisms, both involve the toxin interacting with the cellular membrane, adopting a conformation suitable for perforating the cell, and orienting the hydrophobic portion of the molecule into the membrane to create the pore. Similarly, it has been proposed that oligomers of misfolded proteins with high solvent-exposed hydrophobicity embed within the cellular membrane[16,39,47,48] and disrupt membrane integrity and ion homeostasis.[49] That claramine is efficacious against both melittin and α-hemolysin suggests that it may also protect against misfolded oligomer cytotoxicity, a proposition that is strengthened by the efficacy of similar aminosterols against misfolded protein oligomers in our previous work.[13,14,18,19]

The protective effect of claramine against the cytotoxicity of pore-forming proteins may stem from the results of interactions between steroid polyamines and the cellular membrane, which result in a modification of the physicochemical properties in such a manner as to make them more resistant to certain types of toxins. The related aminosterol trodusquemine binds within seconds to cells and modifies phospholipid bilayers by decreasing the overall negative charge of the polar region, increasing the mechanical resistance of the bilayer and changing the distribution of lipids within the membrane.[12] Previous research suggests that melittin is preferentially adsorbed onto negatively charged membranes due to electrostatic binding, thus offering a potential explanation to the near-full recovery and protection of cells treated with claramine.[50,51] These points are relevant because the mechanism of toxicity for both misfolded protein oligomers and pore-forming toxins involves the mechanical insertion of the hydrophobic region into the bilayer. The misfolded oligomer of the Aβ42 peptide that plays a key role as a toxic agent in Alzheimer's disease, as well as of other protein fragments that damage cell health in other protein misfolding diseases such as bovine spongiform encephalopathy and Parkinson's disease, can function by permeabilizing cellular membranes.[52,53] This perturbation of lipid homeostasis by

membrane-disrupting proteins and macromolecules is known to be attenuated by the modifications caused by trodusquemine.[12] Indeed, this therapeutic approach may offer utility in overcoming the membrane-disrupting properties of misfolded protein oligomers, which have been shown to include pore formation for Aβ and islet amyloid polypeptide (IAPP).[54,55] Based on the concept that unregulated ion homeostasis, protein aggregation, and membrane disruption all contribute to a self-propagating feedback loop that enhances the toxicity of protein aggregation,[56] our findings collectively suggest that aminosterols can modulate the membrane to slow or arrest the cytotoxicity of misfolded oligomers and other faster-acting biological toxins. The role of divalent metals, such as Ca^{2+} ions that are known to play a role in fibril formation and oligomer-induced membrane damage,[56] is a topic worth exploring systematically in future studies to gain further insight into the mechanism of this family of cell membrane protectors.

The generic mechanism by which claramine abrogates the cytotoxicity of pore-forming agents and misfolded protein aggregates suggests that this and related steroid polyamines may be broadly applicable as a countermeasure against biological threat agents by regulating the lipid content of the membrane. While melittin and α-hemolysin do not form toxic aggregates through misfolded intermediates as is the case for protein aggregation processes linked to neurodegenerative diseases, these results suggest that claramine may prevent the toxicity of other biomolecules that target cell membranes. We propose that this aminosterol integrates into the broader lipid homeostasis system, which dynamically modulates the synthesis, trafficking, concentrations, interactions, and destruction of lipids in real time,[57,58] to modulate the physical state of lipid membranes and safeguard against toxic insult by preventing biomolecule-induced damage to lipid membranes or by enabling membrane repair mechanisms that can restore lipid and cellular homeostasis.[2] For example, diphtheria toxin and the lethal factor of anthrax are transmitted into the cytosol via a pore-forming protein, which inserts into the cellular membrane.[59,60] The generic process of pore formation shown by a number of biological threat agents indicates that claramine and other aminosterols may be effective at protecting cells from deadly toxins. Moreover, trodusquemine has been shown to induce the redistribution of GM1 and cholesterol molecules,[12] two critical lipids abundant in lipid rafts that are ubiquitous in neuronal membranes.[61] Alterations in such membrane regions have been linked to neuronal dysfunction and neurodegenerative diseases,[12,62] and it is possible that aminosterols regulate the lipid content of the cell in its ability to protect against the damage induced by a variety of toxins.

The physicochemical changes induced by claramine and other aminosterols to the cellular membrane could also protect cells experiencing other forms of membrane stress. For example, the lipid membranes of skeletal muscle cells are prone to increased permeability after eccentric contractions, forming membrane ruptures large enough to release creatine phosphokinase.[2,63] This is similar to the effect of various genetic muscular dystrophy diseases, wherein plasma membranes of muscle cells are weaker than normal and more prone to rupture under mechanical stress.[2] Since aminosterols increase the resistance of cellular membranes to mechanical stress,[12] they may be effective at improving the condition of muscular cells weakened either through overuse or genetic abnormalities. Moreover, the effectiveness of claramine against

α-hemolysin toxicity in vitro suggests that it may aid in the treatment of methicillin-resistant *S. aureus* (MRSA) by attenuating this virulence factor. Finally, squalamine[64] and trodusquemine[65] have been utilized in a variety of clinical trials and demonstrated advantageous pharmacokinetic properties and safety profiles, which suggests that claramine may also demonstrate similar properties owing to its high degree of structural similarity to these aminosterols. Moreover, claramine can be delivered to the brain via intranasal administration,[66] and the aminosterol trodusquemine has also been reported to cross the blood−brain barrier.[15]

In conclusion, these findings collectively show that claramine is a potent molecule for protecting cells from membrane-disrupting toxins. As aminosterols have been shown to bind cell membranes, making them less negatively charged inducing a redistribution of cholesterol and ganglioside GM1 molecules and making them more resistant to indentation or oligomer embedding,[12] this and other aminosterols may offer a unique therapeutic approach to protect the plasma membrane of cells from a wide range of toxic biomolecules implicit in numerous human pathologies.

■ METHODS

Reagents. Claramine trifluoroacetate salt (>98%) was acquired from Sigma-Aldrich (MO) and its identity was confirmed by mass spectrometry. Aliquots were prepared at a concentration of 1 mM in water and stored at −20 °C. Melittin (>85%) was acquired from Sigma-Aldrich (MO), and aliquots were prepared at a concentration of 1 mM in water and stored at −20 °C. α-Hemolysin (>60% protein by Lowry, ≥10,000 units/mg protein) was acquired from Sigma-Aldrich (MO), and aliquots were prepared at a concentration of 500 μg/mL in water and stored at −20 °C. Samples containing pore-forming agents were handled and disposed of with care and according to the manufactuer's recommendations and guidelines. All samples containing proteins were prepared or stored in Eppendorf LoBind Tubes (Hamburg, Germany).

Cell Culture. Human SH-SY5Y neuroblastoma cells (ATCC, VA) were cultured in Dulbecco's modified Eagle's medium (DMEM)/F-12 with L-glutamine, N-(2-hydroxyethyl)piperazine-N′-ethanesulfonic acid (HEPES), and phenol red (11330032, ThermoFisher Gibco, MA) and supplemented with 10% fetal bovine serum (FBS) and 1.0% antibiotics (penicillin−streptomycin, ThermoFisher Gibco, MA). Cell cultures were maintained in a 5% CO$_2$-humidified atmosphere at 37 °C and grown until they reached 80% confluence for a maximum of 20 passages.[15,67] The cell line was authenticated and tested negative for mycoplasma contamination. Human HEK293 embryonic kidney cells were cultured under the same conditions.

MTT Reduction Assay. Melittin (2 μM, in monomer equivalents) or α-hemolysin (50 μg/mL corresponding to ca. 1.5 μM, in monomer equivalents) were added to the cell culture media and incubated with or without increasing concentrations of CL for 1 h at 37 °C under quiescent conditions. After this incubation, the culture media of cells seeded in 96-well plates was replaced with the aforementioned solutions containing melittin and claramine for 20 h or 30 min, as indicated in the text. Following treatment of the cells, the 3-(4,5-dimethylthiazol-2-yl)-2,5-diphenyltetrazolium bromide (MTT, purchased from Sigma-Aldrich, MO) reduction assay was performed as previously described.[68]

Brightfield Images. Cells were treated with melittin or α-hemolysin as described, and the various conditions were imaged using a Motic AE31E inverted microscope and a Jenoptix Gryphax microscope camera (Jena, Germany). Scale bars for all cell images were estimated based on the width of typical SH-SY5Y cells.

Trypan Blue Exclusion Assays. Cells were detached using trypsin and diluted in aliquots to 200,000 cells/mL. Cells in suspension were then exposed to 4 μM melittin in the absence or presence of 5 or 10 μM CL. The extent of trypan blue (0.4% trypan

blue stain, T10282, Invitrogen, CA) exclusion was monitored at 10 and 40 min of incubation using a Countess II automated cell counter (ThermoFisher Applied Biosystems, CA).

Measurement of Intracellular ROS. Melittin (0.1 μM, monomer equivalents) or α-hemolysin (50 μg/mL, monomer equivalents) were added to the cell culture media of SH-SY5Y cells seeded on glass coverslips (Corning BioCoat Poly-D-Lysin/Laminin, NY) for 5 or 1 min, respectively, in the absence or presence of 0.01–10 μM claramine. To detect intracellular ROS production, cells were loaded with 10 μM 6-chloromethyl-2′,7′-dichlorodihydrofluorescein diacetate (CM-H$_2$DCFDA, Life Technologies, CA) during the aforementioned treatment. The resulting fluorescence was analyzed by a Nikon C2 scanning laser confocal microscopy system (Nikon Instruments, NY). A series of 1.0 μm thick optical sections (1024 × 1024 or 2048 × 2048) were taken through the cells using a Nikon Eclipse Ti inverted microscope (Nikon Instruments) equipped with a 60× oil immersion objective (Nikon Instruments) and then projected as a single composite image by superimposition. The confocal microscope was set at optimal acquisition conditions, e.g., pinhole diameters, detector gain, and laser powers. Settings were maintained constant for all image acquisitions. For Figures 1C and 3B, the same images are shown with enhanced brightness and contrast such that all cells can be visualized (Figure S9), including those with low fluorescence signals.

Melittin Binding to the Cellular Membrane. To label melittin, 300 μM Alexa Fluor 488 N-hydroxysuccinimide (NHS) ester (succinimidyl ester, Invitrogen, ThermoFisher Scientific, CA) was incubated with gentle shaking for 2 h with 900 μM melittin in 0.1 mM sodium bicarbonate buffer (pH 8.0, Sigma-Aldrich, MO). SH-SY5Y cells were seeded on glass coverslips (Corning BioCoat Poly-D-Lysin/Laminin, NY) and treated for 5 min with 0.2 μM labeled melittin in the absence or presence of 0.1, 1.0, and 10 μM claramine. After incubation, the cells were washed with phosphate-buffered saline (PBS) and counterstained with 5 μg/mL Alexa Fluor 633-conjugated wheat germ agglutinin (Life Technologies, CA).[13] After washing with PBS, cells were fixed in 2% paraformaldehyde. Fluorescence emission was detected after double excitation at 488 and 633 nm by the above-described scanning confocal microscopy system using a 60× oil immersion objective (Nikon Instruments). A series of 1.0 μm thick optical sections (1024 × 1024) were acquired, and all sections were projected as a single composite image by superimposition. ImageJ (NIH, Bethesda, MD) was used to calculate the percentage of colocalization between cell membranes and melittin.

α-Hemolysin Binding to the Cellular Membrane. SH-SY5Y cells were seeded on glass coverslips (Corning) and treated for 15 min with 5 μg/mL (e.g., about 0.15 μM in monomer equivalents) of α-hemolysin in the absence or presence of 0.1 and 10 μM claramine. After incubation, the cells were washed with PBS, counterstained with 10 μg/ml Alexa Fluor 633-conjugated wheat germ agglutinin (Life Technologies, CA),[13] and fixed in 2% paraformaldehyde. After washing with PBS, the presence of α-hemolysin was detected with 1:750 diluted rabbit antistaphylococcal α-toxin primary antibodies (Sigma-Aldrich, MO) and subsequently with 1:1000 diluted Alexa Fluor 488-conjugated antirabbit secondary antibodies (Life Technologies, CA). Fluorescence emission was detected after double excitation at 488 and 633 nm by the above-described scanning confocal microscopy system using a 20× objective (Nikon Instruments). A series of 1.0 μm thick optical sections (1024 × 1024) were acquired, and all sections were projected as a single composite image by superimposition. ImageJ (NIH, Bethesda, MD) was used to calculate the percentage of colocalization between cell membranes and α-hemolysin.

Circular Dichroism Spectroscopy. Samples containing 10 μM melittin in the absence and presence of up to 30 μM CL were prepared in 20 mM sodium phosphate buffer, pH 7.4. Scans were acquired at 25 °C, 50 nm/min, over 20 accumulations with a data pitch of 0.5 nm. A smoothing function was applied to the mean residue ellipticity plot, and the BeStSel model[35,36] was used to quantify the secondary structure of MEL.

ANS Binding Measurements. Solutions with melittin (10 μM) or α-hemolysin (100 μg/mL) in buffer (20 mM sodium phosphate buffer at pH 7.4) were aliquoted after incubation for 1 h in the absence or presence of CL up to 30 μM and 8-anilinonaphthalene-1-sulfonate (ANS, Sigma-Aldrich, MO) was subsequently added from a 1 mM concentrated stock. Emission spectra were recorded using a plate reader (BioTek Synergy H1, VT) with excitation at 380 nm. Spectra were background-subtracted to that of the spectra of buffer alone.

Turbidity Measurements. The same samples from the ANS preparation were analyzed for absorbance using a plate reader (BioTek Synergy H1, VT) with spectral scanning. With the CD, ANS, and turbidity measurements, we elected to probe only up to 30 μM given that 40 and 50 μM concentrations of claramine in the absence of melittin caused an increase in ANS fluorescence intensity in the absence of a blue shift, indicating that there may be an avidity effect between claramine and ANS at such high concentrations, while concentrations of claramine at and below 30 μM did not clearly change the signal of free ANS or its absorbance (Figure S10). We note that it was necessary to use a 5-fold greater concentration of melittin in these in vitro measurements in comparison to the tissue culture experiments to resolve a sufficient and reproducible signal from the peptide alone.

Atomic Force Microscopy (AFM) of Melittin. As mica carries a negative charge, and therefore only positively charged molecules are easily absorbed,[69] we expected and experimentally observed binding of the cationic peptide melittin to bare mica without functionalization. AFM sample deposition was carried out at room temperature by depositing a 10 μL drop of protein at a concentration of 2 μM for 2 min to a freshly cleaved mica surface (AGF7013, Agar Scientific, Essex, U.K.). After deposition, salt from the 20 mM sodium phosphate buffer was washed away with Elga purified water (Purelab Classic, model CLXXXUFM2-US) and samples were stored in a sealed container until imaging using a Bruker Multimode 8 AFM (MA) in tapping mode with scan rates <0.5 Hz and a silicon tip with an 8 nm nominal radius (model RSTEP, MPP-11100, Bruker, MA).

Statistics. Data were analyzed using GraphPad Prism 9 (CA) using an unpaired, two-tailed Student's t-test, two-way ANOVA, or one-way ANOVA followed by Dunnett's postcomparison test relative to untreated cells or samples containing pore-forming peptides, as indicated in the corresponding figure legends.

■ ASSOCIATED CONTENT

ⓢ Supporting Information

The Supporting Information is available free of charge at https://pubs.acs.org/doi/10.1021/acschemneuro.1c00840.

> Experiments to determine the concentrations of melittin and claramine that are amenable to cells (Figure S1), additional toxicity assays and cell images (Figures S2–S5), cytotoxicity experiments in kidney cells (Figure S6), biophysical experiments with α-HEM (Figure S7), control experiments for the toxicity of Alexa-labeled melittin (Figure S8), enhanced brightness images of Figues 1C and 3B (Figure S9), and controls for in vitro biophysical experiments (Figure S10) (PDF)

■ AUTHOR INFORMATION

Corresponding Authors

Michele Vendruscolo — *Centre for Misfolding Diseases, Yusuf Hamied Department of Chemistry, University of Cambridge, Cambridge CB2 1EW, U.K.;* ⓞ orcid.org/0000-0002-3616-1610; Email: mv245@cam.ac.uk

Ryan Limbocker — *Department of Chemistry and Life Science, United States Military Academy, West Point, New York 10996, United States;* ⓞ orcid.org/0000-0002-6030-6656; Email: ryan.limbocker@westpoint.edu

Authors

Ryan P. Kreiser − *Department of Chemistry and Life Science, United States Military Academy, West Point, New York 10996, United States*

Aidan K. Wright − *Department of Chemistry and Life Science, United States Military Academy, West Point, New York 10996, United States*

Liam R. Sasser − *Department of Chemistry and Life Science, United States Military Academy, West Point, New York 10996, United States*

Dillon J. Rinauro − *Centre for Misfolding Diseases, Yusuf Hamied Department of Chemistry, University of Cambridge, Cambridge CB2 1EW, U.K.*

Justus M. Gabriel − *Department of Chemistry and Life Science, United States Military Academy, West Point, New York 10996, United States*

Claire M. Hsu − *Department of Chemistry and Life Science, United States Military Academy, West Point, New York 10996, United States*

Jorge A. Hurtado − *Department of Chemistry and Life Science, United States Military Academy, West Point, New York 10996, United States*

Tristan L. McKenzie − *Department of Chemistry and Life Science, United States Military Academy, West Point, New York 10996, United States*

Silvia Errico − *Centre for Misfolding Diseases, Yusuf Hamied Department of Chemistry, University of Cambridge, Cambridge CB2 1EW, U.K.; Department of Experimental and Clinical Biomedical Sciences, University of Florence, Florence 50134, Italy;* orcid.org/0000-0001-6197-9740

J. Alex Albright − *Department of Chemistry and Life Science, United States Military Academy, West Point, New York 10996, United States*

Lance Richardson − *Department of Chemistry and Life Science, United States Military Academy, West Point, New York 10996, United States*

Victor A. Jaffett − *Department of Chemistry and Life Science, United States Military Academy, West Point, New York 10996, United States*

Dawn E. Riegner − *Department of Chemistry and Life Science, United States Military Academy, West Point, New York 10996, United States;* orcid.org/0000-0002-0283-0652

Lam T. Nguyen − *Department of Chemistry and Life Science, United States Military Academy, West Point, New York 10996, United States*

Kathleen LeForte − *Department of Chemistry and Life Science, United States Military Academy, West Point, New York 10996, United States*

Michael Zasloff − *MedStar-Georgetown Transplant Institute, Georgetown University School of Medicine, Washington, District of Columbia 20010, United States;* orcid.org/0000-0002-1453-9328

Jared E. Hollows − *Department of Chemistry and Life Science, United States Military Academy, West Point, New York 10996, United States*

Fabrizio Chiti − *Department of Experimental and Clinical Biomedical Sciences, University of Florence, Florence 50134, Italy;* orcid.org/0000-0002-1330-1289

Complete contact information is available at:
https://pubs.acs.org/10.1021/acschemneuro.1c00840

■ REFERENCES

(1) Nicolson, G. L. Cell Membrane Fluid−Mosaic Structure and Cancer Metastasis. *Cancer Res.* **2015**, *75*, 1169−1176.

(2) Dias, C.; Nylandsted, J. Plasma Membrane Integrity in Health and Disease: Significance and Therapeutic Potential. *Cell Discovery* **2021**, *7*, No. 4.

(3) Draeger, A.; Monastyrskaya, K.; Babiychuk, E. B. Plasma Membrane Repair and Cellular Damage Control: The Annexin Survival Kit. *Biochem. Pharmacol.* **2011**, *81*, 703−712.

(4) van Meer, G.; Voelker, D. R.; Feigenson, G. W. Membrane Lipids: Where They Are and How They Behave. *Nat. Rev. Mol. Cell Biol.* **2008**, *9*, 112−124.

(5) Bruce, K. D.; Zsombok, A.; Eckel, R. H. Lipid Processing in the Brain: A Key Regulator of Systemic Metabolism. *Front. Endocrinol.* **2017**, *8*, No. 60.

(6) Sastry, P. S. Lipids of Nervous Tissue: Composition and Metabolism. *Prog. Lipid Res.* **1985**, *24*, 69−176.

(7) Kao, Y.-C.; Ho, P.-C.; Tu, Y.-K.; Jou, I.-M.; Tsai, K.-J. Lipids and Alzheimer's Disease. *Int. J. Mol. Sci.* **2020**, *21*, No. 1505.

(8) Young, S. A.; Mina, J. G.; Denny, P. W.; Smith, T. K. Sphingolipid and Ceramide Homeostasis: Potential Therapeutic Targets. *Biochem. Res. Int.* **2012**, *2012*, No. 248135.

(9) Gibson Wood, W.; Eckert, G. P.; Igbavboa, U.; Müller, W. E. Amyloid Beta-Protein Interactions with Membranes and Cholesterol: Causes or Casualties of Alzheimer's Disease. *Biochim. Biophys. Acta, Biomembr.* **2003**, *1610*, 281−290.

(10) Habchi, J.; Chia, S.; Galvagnion, C.; Michaels, T. C. T.; Bellaiche, M. M. J.; Ruggeri, F. S.; Sanguanini, M.; Idini, I; Kumita, J. R.; Sparr, E.; Linse, S.; Dobson, C. M.; Knowles, T. P. J.; Vendruscolo, M. Cholesterol Catalyses Aβ42 Aggregation through a Heterogeneous Nucleation Pathway in the Presence of Lipid Membranes. *Nat. Chem.* **2018**, *10*, 673−683.

(11) Evangelisti, E.; Cascella, R.; Becatti, M.; Marrazza, G.; Dobson, C. M.; Chiti, F.; Stefani, M.; Cecchi, C. Binding Affinity of Amyloid Oligomers to Cellular Membranes Is a Generic Indicator of Cellular Dysfunction in Protein Misfolding Diseases. *Sci. Rep.* **2016**, *6*, No. 32721.

(12) Errico, S.; Lucchesi, G.; Odino, D.; Muscat, S.; Capitini, C.; Bugelli, C.; Canale, C.; Ferrando, R.; Grasso, G.; Barbut, D.; Calamai, M.; Danani, A.; Zasloff, M.; Relini, A.; Caminati, G.; Vendruscolo, M.; Chiti, F. Making Biological Membrane Resistant to the Toxicity of Misfolded Protein Oligomers: A Lesson from Trodusquemine. *Nanoscale* **2020**, *12*, 22596−22614.

(13) Perni, M.; Galvagnion, C.; Maltsev, A.; Meisl, G.; Müller, M. B. D.; Challa, P. K.; Kirkegaard, J. B.; Flagmeier, P.; Cohen, S. I. A.; Cascella, R.; Chen, S. W.; Limbocker, R.; Sormanni, P.; Heller, G. T.; Aprile, F. A.; Cremades, N.; Cecchi, C.; Chiti, F.; Nollen, E. A. A.; Knowles, T. P. J.; Vendruscolo, M.; Bax, A.; Zasloff, M.; Dobson, C. M. A Natural Product Inhibits the Initiation of α-Synuclein Aggregation and Suppresses Its Toxicity. *Proc. Natl. Acad. Sci. U.S.A.* **2017**, *114*, E1009−E1017.

(14) Perni, M.; Flagmeier, P.; Limbocker, R.; Cascella, R.; Aprile, F. A.; Galvagnion, C.; Heller, G. T.; Meisl, G.; Chen, S. W.; Kumita, J. R.; Challa, P. K.; Kirkegaard, J. B.; Cohen, S. I. A.; Mannini, B.; Barbut, D.; Nollen, E. A. A.; Cecchi, C.; Cremades, N.; Knowles, T. P. J.; Chiti, F.; Zasloff, M.; Vendruscolo, M.; Dobson, C. M. Multistep Inhibition of α-Synuclein Aggregation and Toxicity in Vitro and in Vivo by Trodusquemine. *ACS Chem. Biol.* **2018**, *13*, 2308−2319.

(15) Limbocker, R.; Chia, S.; Ruggeri, F. S.; Perni, M.; Cascella, R.; Heller, G. T.; Meisl, G.; Mannini, B.; Habchi, J.; Michaels, T. C. T.; Challa, P. K.; Ahn, M.; Casford, S. T.; Fernando, N.; Xu, C. K.; Kloss, N. D.; Cohen, S. I. A.; Kumita, J. R.; Cecchi, C.; Zasloff, M.; Linse, S.; Knowles, T. P. J.; Chiti, F.; Vendruscolo, M.; Dobson, C. M. Trodusquemine Enhances Aβ42 Aggregation but Suppresses Its Toxicity by Displacing Oligomers from Cell Membranes. *Nat. Commun.* **2019**, *10*, No. 225.

(16) Kreiser, R. P.; Wright, A. K.; Block, N. R.; Hollows, J. E.; Nguyen, L. T.; LeForte, K.; Mannini, B.; Vendruscolo, M.; Limbocker, R. Therapeutic Strategies to Reduce the Toxicity of Misfolded Protein Oligomers. *Int. J. Mol. Sci.* **2020**, *21*, No. 8651.

(17) Limbocker, R.; Mannini, B.; Cataldi, R.; Chhangur, S.; Wright, A. K.; Kreiser, R. P.; Albright, J. A.; Chia, S.; Habchi, J.; Sormanni, P.; Kumita, J. R.; Ruggeri, F. S.; Dobson, C. M.; Chiti, F.; Aprile, F. A.; Vendruscolo, M. Rationally Designed Antibodies as Research Tools to Study the Structure−Toxicity Relationship of Amyloid-β Oligomers. *Int. J. Mol. Sci.* **2020**, *21*, No. 4542.

(18) Limbocker, R.; Mannini, B.; Ruggeri, F. S.; Cascella, R.; Xu, C. K.; Perni, M.; Chia, S.; Chen, S. W.; Habchi, J.; Bigi, A.; Kreiser, R. P.; Wright, A. K.; Albright, J. A.; Kartanas, T.; Kumita, J. R.; Cremades, N.; Zasloff, M.; Cecchi, C.; Knowles, T. P. J.; Chiti, F.; Vendruscolo, M.; Dobson, C. M. Trodusquemine Displaces Protein Misfolded Oligomers from Cell Membranes and Abrogates Their Cytotoxicity through a Generic Mechanism. *Commun. Biol.* **2020**, *3*, No. 435.

(19) Limbocker, R.; Staats, R.; Chia, S.; Ruggeri, F. S.; Mannini, B.; Xu, C. K.; Perni, M.; Cascella, R.; Bigi, A.; Sasser, L. R.; Block, N. R.; Wright, A. K.; Kreiser, R. P.; Custy, E. T.; Meisl, G.; Errico, S.; Habchi, J.; Flagmeier, P.; Kartanas, T.; Hollows, J. E.; Nguyen, L. T.; LeForte, K.; Barbut, D.; Kumita, J. R.; Cecchi, C.; Zasloff, M.; Knowles, T. P. J.; Dobson, C. M.; Chiti, F.; Vendruscolo, M. Squalamine and Its Derivatives Modulate the Aggregation of Amyloid-β and α-Synuclein and Suppress the Toxicity of Their Oligomers. *Front. Neurosci.* **2021**, *15*, No. 680026.

(20) Perni, M.; van der Goot, A.; Limbocker, R.; van Ham, T. J.; Aprile, F. A.; Xu, C. K.; Flagmeier, P.; Thijssen, K.; Sormanni, P.; Fusco, G.; Chen, S. W.; Challa, P. K.; Kirkegaard, J. B.; Laine, R. F.; Ma, K. Y.; Müller, M. B. D.; Sinnige, T.; Kumita, J. R.; Cohen, S. I. A.; Seinstra, R.; Kaminski Schierle, G. S.; Kaminski, C. F.; Barbut, D.; De Simone, A.; Knowles, T. P. J.; Zasloff, M.; Nollen, E. A. A.; Vendruscolo, M.; Dobson, C. M. Comparative Studies in the A30P and A53T α-Synuclein *C. elegans* Strains to Investigate the Molecular Origins of Parkinson's Disease. *Front. Cell Dev. Biol.* **2021**, *9*, No. 552549.

(21) Errico, S.; Ramshini, H.; Capitini, C.; Canale, C.; Spaziano, M.; Barbut, D.; Calamai, M.; Zasloff, M.; Oropesa-Nuñez, R.; Vendruscolo, M.; Chiti, F. Quantitative Measurement of the Affinity of Toxic and Nontoxic Misfolded Protein Oligomers for Lipid Bilayers and of Its Modulation by Lipid Composition and Trodusquemine. *ACS Chem. Neurosci.* **2021**, *12*, 3189−3202.

(22) Limbocker, R.; Errico, S.; Barbut, D.; J Knowles, T. P.; Vendruscolo, M.; Chiti, F.; Zasloff, M. Squalamine and Trodusquemine: Two Natural Products for Neurodegenerative Diseases, from Physical Chemistry to the Clinic. *Nat. Prod. Rep.* **2022**, DOI: 10.1039/D1NP00042J.

(23) Choi, J. H.; Jang, A. Y.; Lin, S.; Lim, S.; Kim, D.; Park, K.; Han, S.-M.; Yeo, J.-H.; Seo, H. S. Melittin, a Honeybee Venom-Derived Antimicrobial Peptide, May Target Methicillin-Resistant *Staphylococcus aureus*. *Mol. Med. Rep.* **2015**, *12*, 6483−6490.

(24) Park, S.-C.; Kim, J.-Y.; Shin, S.-O.; Jeong, C.-Y.; Kim, M.-H.; Shin, S. Y.; Cheong, G.-W.; Park, Y.; Hahm, K.-S. Investigation of Toroidal Pore and Oligomerization by Melittin Using Transmission Electron Microscopy. *Biochem. Biophys. Res. Commun.* **2006**, *343*, 222−228.

(25) Lee, M.-T.; Sun, T.-L.; Hung, W.-C.; Huang, H. W. Process of Inducing Pores in Membranes by Melittin. *Proc. Natl. Acad. Sci. U.S.A.* **2013**, *110*, 14243−14248.

(26) Sun, D.; Forsman, J.; Woodward, C. E. Multistep Molecular Dynamics Simulations Identify the Highly Cooperative Activity of Melittin in Recognizing and Stabilizing Membrane Pores. *Langmuir* **2015**, *31*, 9388−9401.

(27) van den Bogaart, G.; Guzmán, J. V.; Mika, J. T.; Poolman, B. On the Mechanism of Pore Formation by Melittin. *J. Biol. Chem.* **2008**, *283*, 33854−33857.

(28) Song, L.; Hobaugh, M. R.; Shustak, C.; Cheley, S.; Bayley, H.; Gouaux, J. E. Structure of Staphylococcal α-Hemolysin, a Heptameric Transmembrane Pore. *Science* **1996**, *274*, 1859−1865.

(29) Bhakdi, S.; Tranum-Jensen, J. Alpha-Toxin of *Staphylococcus aureus*. *Microbiol. Rev.* **1991**, *55*, 733−751.

(30) Bhakdi, S.; Mackman, N.; Menestrina, G.; Gray, L.; Hugo, F.; Seeger, W.; Holland, I. B. The Hemolysin of *Escherichia coli*. *Eur. J. Epidemiol.* **1988**, *4*, 135−143.

(31) Vesper, S. J.; Jo Vesper, M. Possible Role of Fungal Hemolysins in Sick Building Syndrome. *Advances in Applied Microbiology*; Academic Press, 2004; Vol. 55, pp 191−213.

(32) Chalmeau, J.; Monina, N.; Shin, J.; Vieu, C.; Noireaux, V. α-Hemolysin Pore Formation into a Supported Phospholipid Bilayer Using Cell-Free Expression. *Biochim. Biophys. Acta, Biomembr.* **2011**, *1808*, 271−278.

(33) Dahlberg, D.; Mariussen, E.; Goverud, I. L.; Tønjum, T.; Mæhlen, J.; Antal, E.-A.; Hassel, B. Staphylococcal α-Hemolysin Is Neurotoxic and Causes Lysis of Brain Cells in Vivo and in Vitro. *Neurotoxicology* **2015**, *48*, 61−67.

(34) Halder, A.; Karmakar, S. An Evidence of Pores in Phospholipid Membrane Induced by an Antimicrobial Peptide NK-2. *Biophys. Chem.* **2022**, *282*, No. 106759.

(35) Micsonai, A.; Wien, F.; Kernya, L.; Lee, Y.-H.; Goto, Y.; Réfrégiers, M.; Kardos, J. Accurate Secondary Structure Prediction and Fold Recognition for Circular Dichroism Spectroscopy. *Proc. Natl. Acad. Sci. U.S.A.* **2015**, *112*, E3095−E3103.

(36) Micsonai, A.; Wien, F.; Bulyáki, É.; Kun, J.; Moussong, É.; Lee, Y.-H.; Goto, Y.; Réfrégiers, M.; Kardos, J. BeStSel: A Web Server for Accurate Protein Secondary Structure Prediction and Fold Recognition from the Circular Dichroism Spectra. *Nucleic Acids Res.* **2018**, *46*, W315−W322.

(37) Mannini, B.; Mulvihill, E.; Sgromo, C.; Cascella, R.; Khodarahmi, R.; Ramazzotti, M.; Dobson, C. M.; Cecchi, C.; Chiti, F. Toxicity of Protein Oligomers Is Rationalized by a Function Combining Size and Surface Hydrophobicity. *ACS Chem. Biol.* **2014**, *9*, 2309−2317.

(38) Cascella, R.; Conti, S.; Mannini, B.; Li, X.; Buxbaum, J. N.; Tiribilli, B.; Chiti, F.; Cecchi, C. Transthyretin Suppresses the Toxicity of Oligomers Formed by Misfolded Proteins in Vitro. *Biochim. Biophys. Acta, Mol. Basis Dis.* **2013**, *1832*, 2302−2314.

(39) Campioni, S.; Mannini, B.; Zampagni, M.; Pensalfini, A.; Parrini, C.; Evangelisti, E.; Relini, A.; Stefani, M.; Dobson, C. M.; Cecchi, C.; Chiti, F. A Causative Link between the Structure of

Aberrant Protein Oligomers and Their Toxicity. *Nat. Chem. Biol.* **2010**, *6*, 140−147.

(40) Zarrinnahad, H.; Mahmoodzadeh, A.; Hamidi, M. P.; Mahdavi, M.; Moradi, A.; Bagheri, K. P.; Shahbazzadeh, D. Apoptotic Effect of Melittin Purified from Iranian Honey Bee Venom on Human Cervical Cancer HeLa Cell Line. *Int. J. Pept. Res. Ther.* **2018**, *24*, 563−570.

(41) Lee, M.-T.; Hung, W.-C.; Chen, F.-Y.; Huang, H. W. Mechanism and Kinetics of Pore Formation in Membranes by Water-Soluble Amphipathic Peptides. *Proc. Natl. Acad. Sci. U.S.A.* **2008**, *105*, 5087−5092.

(42) Bhunia, A.; Domadia, P. N.; Bhattacharjya, S. Structural and Thermodynamic Analyses of the Interaction between Melittin and Lipopolysaccharide. *Biochim. Biophys. Acta, Biomembr.* **2007**, *1768*, 3282−3291.

(43) Chen, L.-Y.; Cheng, C.-W.; Lin, J.-J.; Chen, W.-Y. Exploring the Effect of Cholesterol in Lipid Bilayer Membrane on the Melittin Penetration Mechanism. *Anal. Biochem.* **2007**, *367*, 49−55.

(44) Tosteson, M. T.; Holmes, S. J.; Razin, M.; Tosteson, D. C. Melittin Lysis of Red Cells. *J. Membr. Biol.* **1985**, *87*, 35−44.

(45) Schmitt, M.; Schaffrath, R.; Meinhardt, F. *Microbial Protein Toxins*; Topics in Current Genetics; Springer, 2005; pp 133−155.

(46) Berube, B. J.; Wardenburg, J. B. *Staphylococcus aureus α*-Toxin: Nearly a Century of Intrigue. *Toxins* **2013**, *5*, 1140−1166.

(47) Fusco, G.; Chen, S. W.; Williamson, P. T. F.; Cascella, R.; Perni, M.; Jarvis, J. A.; Cecchi, C.; Vendruscolo, M.; Chiti, F.; Cremades, N.; Ying, L.; Dobson, C. M.; Simone, A. D. Structural Basis of Membrane Disruption and Cellular Toxicity by α-Synuclein Oligomers. *Science* **2017**, *358*, 1440−1443.

(48) Ladiwala, A. R. A.; Litt, J.; Kane, R. S.; Aucoin, D. S.; Smith, S. O.; Ranjan, S.; Davis, J.; Nostrand, W. E. V.; Tessier, P. M. Conformational Differences between Two Amyloid β Oligomers of Similar Size and Dissimilar Toxicity. *J. Biol. Chem.* **2012**, *287*, 24765−24773.

(49) Serra-Batiste, M.; Ninot-Pedrosa, M.; Bayoumi, M.; Gairí, M.; Maglia, G.; Carulla, N. Aβ42 Assembles into Specific β-Barrel Pore-Forming Oligomers in Membrane-Mimicking Environments. *Proc. Natl. Acad. Sci. U.S.A.* **2016**, *113*, 10866−10871.

(50) Strömstedt, A. A.; Wessman, P.; Ringstad, L.; Edwards, K.; Malmsten, M. Effect of Lipid Headgroup Composition on the Interaction between Melittin and Lipid Bilayers. *J. Colloid Interface Sci.* **2007**, *311*, 59−69.

(51) Ohki, S.; Marcus, E.; Sukumaran, D. K.; Arnold, K. Interaction of Melittin with Lipid Membranes. *Biochim. Biophys. Acta, Biomembr.* **1994**, *1194*, 223−232.

(52) Lashuel, H. A.; Hartley, D.; Petre, B. M.; Walz, T.; Lansbury, P. T. Amyloid Pores from Pathogenic Mutations. *Nature* **2002**, *418*, 291.

(53) Kawahara, M.; Ohtsuka, I.; Yokoyama, S.; Kato-Negishi, M.; Sadakane, Y. Membrane Incorporation, Channel Formation, and Disruption of Calcium Homeostasis by Alzheimer's β-Amyloid Protein. *Int. J. Alzheimer's Dis.* **2011**, *2011*, No. 304583.

(54) Sciacca, M. F. M.; Kotler, S. A.; Brender, J. R.; Chen, J.; Lee, D.; Ramamoorthy, A. Two-Step Mechanism of Membrane Disruption by Aβ through Membrane Fragmentation and Pore Formation. *Biophys. J.* **2012**, *103*, 702−710.

(55) Brender, J. R.; Salamekh, S.; Ramamoorthy, A. Membrane Disruption and Early Events in the Aggregation of the Diabetes Related Peptide IAPP from a Molecular Perspective. *Acc. Chem. Res.* **2012**, *45*, 454−462.

(56) Sciacca, M. F. M.; Milardi, D.; Messina, G. M. L.; Marletta, G.; Brender, J. R.; Ramamoorthy, A.; La Rosa, C. Cations as Switches of Amyloid-Mediated Membrane Disruption Mechanisms: Calcium and IAPP. *Biophys. J.* **2013**, *104*, 173−184.

(57) Agmon, E.; Stockwell, B. R. Lipid Homeostasis and Regulated Cell Death. *Curr. Opin. Chem. Biol.* **2017**, *39*, 83−89.

(58) Unger, R. H.; Clark, G. O.; Scherer, P. E.; Orci, L. Lipid Homeostasis, Lipotoxicity and the Metabolic Syndrome. *Biochim. Biophys. Acta, Mol. Cell Biol. Lipids* **2010**, *1801*, 209−214.

(59) Tamayo, A. G.; Bharti, A.; Trujillo, C.; Harrison, R.; Murphy, J. R. COPI Coatomer Complex Proteins Facilitate the Translocation of Anthrax Lethal Factor across Vesicular Membranes in Vitro. *Proc. Natl. Acad. Sci. U.S.A.* **2008**, *105*, 5254−5259.

(60) Finkelstein, A. Channels Formed in Phospholipid Bilayer Membranes by Diphtheria, Tetanus, Botulinum and Anthrax Toxin. *J. Physiol.* **1990**, *84*, 188−190.

(61) Schengrund, C.-L. Lipid Rafts: Keys to Neurodegeneration. *Brain Res. Bull.* **2010**, *82*, 7−17.

(62) Malchiodi-Albedi, F.; Contrusciere, V.; Raggi, C.; Fecchi, K.; Rainaldi, G.; Paradisi, S.; Matteucci, A.; Santini, M. T.; Sargiacomo, M.; Frank, C.; Gaudiano, M. C.; Diociaiuti, M. Lipid Raft Disruption Protects Mature Neurons against Amyloid Oligomer Toxicity. *Biochim. Biophys. Acta, Mol. Basis Dis.* **2010**, *1802*, 406−415.

(63) McNeil, P. L.; Khakee, R. Disruptions of Muscle Fiber Plasma Membranes. Role in Exercise-Induced Damage. *Am. J. Pathol.* **1992**, *140*, 1097−1109.

(64) Hao, D.; Hammond, L. A.; Eckhardt, S. G.; Patnaik, A.; Takimoto, C. H.; Schwartz, G. H.; Goetz, A. D.; Tolcher, A. W.; McCreery, H. A.; Mamun, K.; Williams, J. I.; Holroyd, K. J.; Rowinsky, E. K. A Phase I and Pharmacokinetic Study of Squalamine, an Aminosterol Angiogenesis Inhibitor. *Clin. Cancer Res.* **2003**, *9*, 2465−2471.

(65) Genaera Corporation. *A Phase I, Double-Blind, Randomized, Placebo-Controlled Ascending IV Single-Dose Tolerance and Pharmaco-kinetic Study of Trodusquemine in Healthy Volunteers*; Clinical Trial Registration NCT00509132; clinicaltrials.gov, 2008.

(66) Dodd, G. T.; Xirouchaki, C. E.; Eramo, M.; Mitchell, C. A.; Andrews, Z. B.; Henry, B. A.; Cowley, M. A.; Tiganis, T. Intranasal Targeting of Hypothalamic PTP1B and TCPTP Reinstates Leptin and Insulin Sensitivity and Promotes Weight Loss in Obesity. *Cell Rep.* **2019**, *28*, 2905.e5−2922.e5.

(67) Cascella, R.; Perni, M.; Chen, S. W.; Fusco, G.; Cecchi, C.; Vendruscolo, M.; Chiti, F.; Dobson, C. M.; De Simone, A. Probing the Origin of the Toxicity of Oligomeric Aggregates of α-Synuclein with Antibodies. *ACS Chem. Biol.* **2019**, *14*, 1352−1362.

(68) Cascella, R.; Evangelisti, E.; Bigi, A.; Becatti, M.; Fiorillo, C.; Stefani, M.; Chiti, F.; Cecchi, C. Soluble Oligomers Require a Ganglioside to Trigger Neuronal Calcium Overload. *J. Alzheimer's Dis.* **2017**, *60*, 923−938.

(69) Ruggeri, F. S.; Šneideris, T.; Chia, S.; Vendruscolo, M.; Knowles, T. P. J. Characterizing Individual Protein Aggregates by Infrared Nanospectroscopy and Atomic Force Microscopy. *J. Visualized Exp.* **2019**, *151*, No. e60108.